Analyst

Accepted Manuscript

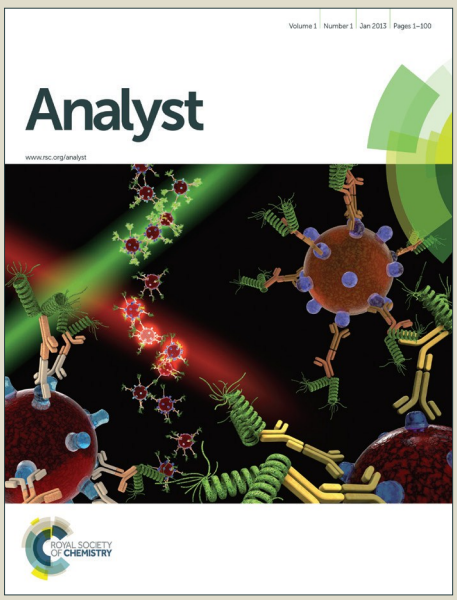

ROYAL SOCIETY OF CHEMISTRY

www.rsc.org/analyst

Real-time quantitative nicking endonuclease-mediated isothermal amplification with small molecular beacons

Wentao Xu[a, b, 1], Chenguang Wang[a, 1], Pengyu Zhu[a,b], Tianxiao Guo[a], Yuancong Xu[a, b], Kunlun Huang[a, b], and Yunbo Luo[a, b, *]

[a] Beijing Advanced Innovation Center for Food Nutrition and Human Health, College of Food Science & Nutritional Engineering, China Agricultural University, Beijing 100083, China

[b]Beijing Laboratory for Food Quality and Safety, College of Food Science and Nutritional Engineering, China Agricultural University, Beijing 100083, China

[1]The two authors contribute equally

*To whom correspondence should be addressed. Tel/Fax: +86 010 62736479; Email: lyb@cau.edu.cn

ABSTRACT

Techniques of isothermal amplification have recently made great strides, and have generated significant interest in the field of point-of-care detection. Nicking endonuclease-mediated isothermal amplification (NEMA) is an example of simple isothermal technology. In this paper, a real-time quantitative nicking endonuclease-mediated isothermal amplification with small molecular beacons (SMB-NEMA) of improved specificity and sensitivity is described. First, we optimized the prohibition of *de novo synthesis* by choosing Nt.BstNBI endonuclease. Second, the whole genome was successfully amplified with Nt.BstNBI (6U), betaine (1M) and trehalose (60mM) for the first time. Third, we achieved 10pg sensitivity for the first time after adding a small molecular beacon that spontaneously undergoes a conformational change when hybridizing to target, and the practical test validated the assay's application. The small molecular beacon has a similar melting temperature to reaction temperature, but is approximately 10bp shorter than length of traditional molecular beacon. A new threshold regulation was also founded for isothermal conditions. Finally, we established a thermodynamic model for designing small molecular beacon. This multistate model is more correct than the traditional algorithm. This theoretical and practical basis will both help us monitor SMB-NEMA in a quantitative way. In summary, our SMB-NEMA method allows the simple, specific and sensitive assessment of isothermal DNA quantification.

Key words: nicking endonuclease-mediated isothermal amplification; small molecular beacons; quantification; thermodynamic basis; quantitative analysis

Introduction

DNA replication in vitro has been used as an effective method in molecular biology research since the 1970s[1]. There are two main issues to overcome in amplification methods. One is the simplicity for point-of-care detection, and the other is the accuracy for real-time quantitative detection. Isothermal amplification, as a solution to the first issue, has been developed over several decades because of its high specificity and unique convenience. Instead of several melting and annealing cycles, isothermal amplification is achieved under a thermal stable temperature for a shorter time than conventional polymerase chain reaction (PCR). This type of amplification has been applied in the point-of-care detection of foodborne pathogens[2], cancer genes[3] and genetically modified organisms (GMOs) [4]. Nicking endonuclease-mediated isothermal amplification (NEMA) is designed and used widely because of its extraordinary advantages. This technology, based on the principle of strand displacement, cleaves only one strand of duplex DNA to amplify in an exponential form via activity of nicking endonuclease activity[5]. Compared with loop-mediated isothermal amplification (LAMP), which is the most popular isothermal technology, NEMA requires only two pairs of ordinary primers, which greatly simplify primer designing work[6]. On the other hand, NEMA is more inhibited to aerosol pollution than that of LAMP by lowing efficiencies. Moreover, NEMA can amplify at most a 400bp product, which is more universal than rolling cycling amplification (RCA), helicase dependent amplification (HDA), nucleic acid sequence-based amplification (NASBA) and other isothermal technologies. Finally, NEMA is stable and inexpensive compared to other isothermal technics [7-9].

However, pollution and low specificity make quantification of NEMA problematic. Considering the complex reaction system that NEMA requires, including two types of enzymes and *de novo synthesis*[10], traditional quantitative methods do not perform well. LAMP stained with fluorescent dye SYBR Green I is the most common assay used to quantify target nucleic acids, but it is not useful in other fields because of the low specificity of the dyes[11]. Fluorescence resonance energy transfer (FRET) has the inherent advantage of high specificity and sensitivity in nucleic acid quantification, and *Taq*man probes have become the international standard detection probe for GMO detection. However, this type of probe cannot be used in the absence of 5' to 3' exonucleases[12], which therefore excludes NEMA. Molecular beacons (MBs), which possess a loop-stem structure, could be used as a type of hairpin-shaped hybridization

probes[13]. MBs function when the sequence of the loop is complementary to the target, leading to the separation of fluorophores and quenchers to emit fluorescence. Quantification of NEMA can be achieved by molecular beacons without a requirement for special enzymes. This method could accomplish real-time measurements of isothermal amplification and allow the calculation of the percentage of the target in the whole products. Most importantly, the method could also be useful in research on kinetic patterns of amplification, critical influential factor identification for isothermal hybridization and one-step isothermal quantitative detection systems, which could also be used in the following detection of genes in living cells. MBs have been used in the scientific research to monitor the short nucleic acid chain, amplifying the signal[14-16]. This technology can also be used to understand the temporal expression of genes *in vivo*, to form a detection signal transformed into other biosensor fields and to initiate signal-amplified amplification for ultrasensitive detection. Attempts to combine MBs and isothermal amplification instead of fluorescence dyes for quantitative detection have not been reported. Considering the small bacterial genome and the versatility of bacterial 16s rDNA in genotyping, this paper focuses on the combination of a small molecular beacon and NEMA to establish a new quantitative detection method that we call SMB-NEMA, based on the amplification of *Bacillus cereus* 16s rDNA. Then the paper identifies some key factors that influence the hybridization of small MBs and the target under unchanged temperature, offering a theoretical guide for SMB-NEMA quantitative detection system that can be used in a number of fields.

Materials and methods

Extraction and quantification of genomic DNA from samples

Bacillus cereus samples (Genbank Acc. No. ATCC 11778) were supplied from our laboratory. Genomic DNA was successfully extracted using the TIANamp Bacteria DNA Kit (Tiangen Biotech Co., Ltd., Beijing, China). DNA was quantified by absorbance at 260 nm using NanoDrop UV spectrophotometry (Thermo Scientific, Massachusetts, USA). Another source of genomic DNA from genetically modified organisms Bt 176 was also prepared like before. To confirm whether the extracted DNA is suitable for the reaction, extracted DNA was followed by the amplification of the 16s rDNA target gene (GenBank Acc. No: NC_016784.1) using 16s-F and 16s-R primers. The PCR procedure was 95°C for 5 min, 95°C for 30 s, 60°C for 1 min, and 72°C for 30 s for 35 cycles, followed by a hold at 72°C for 7 min. Extracted DNA was evaluated by 2% agarose gel electrophoresis. Then, DNA was diluted to several gradients, from 200 ng/μL to 0.001 ng/μL, and stored at -20°C.

Primers and probes design

The primers were designed using Primer Premier 6 software (Premier Biosoft, Palo Alto, USA) and synthesized by Invitrogen Co. Ltd. (Shanghai, China). S_1 and S_2 are located in the region of 16srDNA. Each primer has three sections: the first is a sequence that is complementary to the target; the second is the recognition site for nicking endonuclease, and the last is a protected sequence. B_1 and B_2 are located in the outer region of S_1 and S_2, respectively. Detection target length is 245bp. Molecular beacons for the detection were designed using the Primer Express 3.0 software (Applied Biosystems, Foster City, CA, USA) and synthesized by Takara (TaKaRa Biotech, Dalian, China). They were all labeled by carboxyfluorescein (FAM) at the 5' end region and 4-([4-(dimethylamino) phenyl] azo) benzoic acid (DABCYL) at the 3' end region. The scheme of the NEMA primers and the molecular beacons is shown in Table 1. Other primers and small molecular beacons used in this work are described in Table S1.

Real-time quantitative SMB-NEMA assays

The reactions were performed in a total volume of 25 μL in a S1000 thermal cycler (BioRad, California, USA). For an initial denaturation step, 1μL of 10×ThermoPol buffer (New England Biolabs, Beijing, China), 1.6 μM of each S_1/S_2 primer, 0.2 μM of each B_1/B_2 primer and 1 μL of extracted DNA (from 200 to 0.001 ng/μL, as mentioned above) were incubated at 95°C for 5 min in a final volume of 11 μL. After this step, 1.5 μL of 10×ThermoPol buffer, 4 μL dNTP (TaKaRa Biotech, Dalian, China), 1 mM of Mg^{2+} (TaKaRa Biotech, Dalian, China), 60 mM of trehalose (Sigma-Aldrich, Beijing, China), 1 M of betaine (Sigma-Aldrich, Beijing, China), 2.5 μg of BSA (TaKaRa Biotech, Dalian, China), 3 U of Bst DNA polymerase (New England Biolabs., Beijing, China), 6 U of nicking endonuclease (New England Biolabs., Beijing, China), several amounts of extracted Bt 176 DNA, and different amounts of small molecular beacons (0.2μM, 0.4μM, 0.8μM, 1.2μM) were added to the reaction system, and ddH_2O was added to a final 25 μL. The reaction was performed at 60°C for 50 min, and fluorescence readings were collected every 30 s. All the reactions were performed in the screw type of PCR-tube that was designed by our labortorary (China Patent Application No. 201510293982.2) and produced by Beijing Food Safety Tech. Co, Ltd. (Beijing, China).

For the assay based on SYBR Green dye, the molecular beacon was replaced with 1.25 μL of 20×SYBR Green I (Tiangen Biotech Co., Ltd., Beijing, China). The other reagents and procedures were unchanged.

For specificity verification, primers and small molecular beacon were replaced with mismatched primers and beacon in Table 1 and Table S1. The other reagents and procedures were unchanged.

Conventional quantitative PCR assays

The reactions were performed in a total volume of 25 μL in a S1000 thermal cycler (BioRad, California, USA). The reaction system consists of 1× gene expression master mix (Applied Biosystems, Foster City, CA, USA), 0.4 μM S_1/S_2 primer, several amounts of template DNA. ddH_2O was added to a final 25μL. The reactions were performed at 95°C for 5 min, 40 cycles of 95°C 30 s and 60°C 1 min. Fluorescence were collected at each cycle.

Quantitative analysis

For absolute quantification, a standard curve was built between the logarithm of the initial and the Ct value. Data is also extracted after a new threshold that demonstrates the absolute value of lowest fluorescence was set up. In the SYBR Green dye experiment, a standard curve was built between the logarithm of the initial and the cycle value of the highest fluorescence.

To determine the melting temperature of the primers and molecular beacons, the same reagents were added to the reaction as in the quantitative method did, except for extracted DNA and primers. A long sequence that was complementary to the small molecular beacons or primers was added instead. The reaction was performed at 95°C for 5 min and 60°C for 10 min. Then, the fluorescence data were acquired by integrating the signal over 5 s during a linear temperature transition from 40°C to 95°C at 0.5°C /s. The fluorescence data were converted into melting peaks by software.

Kinetic and thermodynamic research of small molecular beacon in SMB-NEMA

Reactions were performed in a total volume of 25 μL in a S1000 thermal cycler (BioRad, California, USA), except for the template. The beacon was first denatured at 95°C for 5 min. Then, the fluorescence profiles were acquired by integrating the signal at the end of each stage during a linear temperature transition from 25°C to 95°C at 1°C /s for 90 s. The fluorescence data were converted into melting peaks using a software package.

To investigate the molecular beacon-template duplex, the same 25μL reaction system plus different amounts of templates were prepared and data were acquired as before. Ratio of molecular beacon and template ranged from 1:4 to 1:20.

Kinetic and thermodynamic equilibrium analysis

Thermodynamic parameters and secondary structures of all oligonucleotides were calculated using bioinformatics software (http:// mfold.rna.albany.edu/) and established algorithms in a two-state model[21,22]. Melting temperature of each molecular beacon was calculated by using several algorithms, which are listed in Table 2. Free energy of each small molecular beacon was calculated using the multistate model of Bonnet and Preyet[20,23-26]. More details of derivations can be found in Supplementary Information.

Practical samples test

10 samples were collected and tested using SMB-NEMA method, including polluted water from river, foods that out of shelf of life and on sale. Genome extraction and NEMA test are all based on the descriptions above.

Results and Discussion

Optimization of NEMA reaction system

In our SMB-NEMA system, target is first amplified with a single strand displaced by another new strand under stable temperature conditions (step I in Fig. 1). The duplex is then broken by endonuclease recognition site cleavage. Molecular beacons will bind to complementary target, monitoring this exponential process (step III in Fig. 1). Without primer and template, dNTP were used in the template amplification, showing a light but inevitable background. This phenomenon, namely *de novo synthesis*, is negative to the reaction, because we can barely discriminate target from nonspecific background, as shown in Fig. 1(step II in Fig. 1). A real-time fluorescence amplification curve supports our conclusion (Fig. S1). Simulation of *de novo synthesis* gives a later Ct value than normal, though the sigmoidal shape of *de novo synthesis* can also illustrate self-amplification after generation of many palindrome structures. A tendency of amplified potential of negative control could also corroborate our prediction. As we selected two nicking endonucleases that have compatible temperature with reaction temperature, we found that Nt. BstNBI performed well in prohibiting *de novo synthesis*. *De novo synthesis* product amplified in Nt. BstNBI is of longer length than the desired product. Combined with reaction temperature, we then decided to use Nt. BstNBI in our following research (Fig. 2A). We also added betaine and trehalose to help amplify the whole genome based on other reports[27,28]. 1 M betaine and 60 mM trehalose allowed for better performance (Fig. 2B, 2C). The NEMA system was better in *de novo synthesis* prohibition and the whole

genome amplification efficiency when we added 6 U of Nt. BstNBI, 1 M of betaine and 60 mM of trehalose to the original reaction system.

Choice of small molecular beacons that classify as qualitative and quantitative-fitted based on the amplification curve

Different amplifications using small MBs with melting temperature (Tm) ranging from 75°C to 50°C were conducted. An MB with a Tm of 75°C was designed based on the principle of molecular beacons and probes that the melting temperature of the MB is 10-15°C higher than the primer melting temperature[13]. Here we designed a small molecular beacon with a shorter sequence that was complementary to the target. As is shown in Fig. 3, MB with a Tm of 75°C did not have a sigmoidal amplification curve. The separation of loop lasted the entire reaction time. In addition, MBs with Tm higher than the reaction temperature (60°C) did not perform well either. However, these MBs could also be used for qualitative detection, because the curve could be different from the negative control. Thus, we can classify these MBs as qualitative-fitted and quantitative-fitted.

To better identify the quantitative detection dynamic range that these small MBs possessed, the amplification curves were transformed into linear regression curves based on the established amplification theory. Linear between the logarithm of the initial template DNA concentration and the Ct value are shown in Fig. S2. Small MBs with Tm close to the reaction temperature performed well, and MBs with Tm below the reaction temperature had narrow quantification range. In this way, small MBs with Tm above the reaction temperature were qualitative-fitted, whereas small MBs with Tm below the reaction temperature were quantitative-fitted. One important observation was that the fluorescence fluctuated around the threshold at the beginning of the reaction. Ct value was easier to distinguish if we make a new threshold regulation, which will be described later. Small molecular beacon with 60°C Tm was the best choice after we take amplification curve and quantitative dynamic range into consideration, and was used in the following experiments.

Optimization of small molecular beacon addition to the quantitative detection

MBs act as a fluorescence probe to emit a signal when spontaneously binding to the template (step III in Fig. 1). In our study, we selected five dilution series of small MBs, from 0.2 to 1.2 μM. Having chosen small MB of 60°C melting temperature as the fluorescence probe, amplification curve generated after adding various amounts of MBs is shown in Fig. 4. The top fluorescence signal increased evidently with more addition of small MB. However, a larger amount of small MBs could prohibit the reaction, as observed from the later Ct value. A low

dose of small MBs is not enough to distinguish the positive curve from negative control (Fig. 4A), while a high dose of small MBs could also narrow the quantitative range (Fig. 4C, 4D). Thus, the addition of 0.4 μM of small molecular beacon was selected after these two factors were considered comprehensively. In this way, the reaction was finished within 40 min, and the fluorescence signal is suitable for determining effective quantitative amplification.

Specificity improvement in SMB-NEMA

In order to test specificity of our method, two experiments were conducted in SMB-NEMA. Firstly, unrelated templates were added in all reactions mentioned above and gave no positive correspondence. To better prove our specificity improvement under SMB involvement, we then devised several primers and beacons with one base pair mismatch (Sequences can be obtained from Table S1). Based on the well-know theory, primer with 5' single nucleotide polymorphism (SNP) does not influence PCR reaction. As indicated in Fig.S3, all unspecific amplification, no matter which primer and SMB altered and which position mutated, cannot be amplified properly. 5' mismatched primer had little effect on amplification and quantification, which has been in accordance to our hypothesis. Only the right primer and SMB will make correct amplification curve. In this way, specificity in SMB-NEMA has been improved greatly.

Sensitive quantitative detection based on SMB-NEMA

After our previous research, a real-time quantitative SMB-NEMA detection system was finally established (Fig. 5). In the curve, fluorescence was decreased first and turned back to the initial value before exponential or ultra-exponential amplification stage. A possible explanation for this ultra-exponential amplification can be contributed to exponential amplification in the presence of strand that have an enzyme recognition site and nicking endonuclease, as shown in Fig. 1(step III). All these work will greatly improve NEMA specificity and sensitivity. Considering that quantification is based on threshold settlement, we established a new definition of threshold determination: The threshold value is the value back to the initial one. The core of this threshold definition is kinetic of SMB in NEMA reaction and the original description[29]. As fluorescence decreased at first and turned back before exponential amplification, this value is also the fluorescence that returned to the initial value. Considering the dynamic range and linear correlation coefficient (R^2), we now established a specific and sensitive quantitative method (Fig. 5, left bottom). From this curve, we can detect template DNA from 200 ng to 10 pg in the reaction system. Under the algorithm of copy number calculation[30] and the multi-copied number of

target 16s rDNA gene, this system achieved a limit of quantification (LOQ) of 113 copies. This LOQ is comparable to that of LAMP[31], which is a widely used isothermal amplification technology.

Owing to its equivalent or higher specificity and the lack of requirement of thermal cycling compared with conventional PCR, isothermal amplification could be better used in point-of-care detection with an optimized system. Target-based amplification was hardly detected quantitatively in isothermal conditions. Quantification using the SYBR Green fluorescence dye has been reported[31]. However, this quantification is used negatively in other isothermal conditions because SYBR Green dye can bind to all double-stranded DNA, thereby causing false-positive results. For example, as shown in Fig. S4, although NEMA with SYBR Green is consistent with predicted amplification theory of a standard sigmoidal shape, it is unavailable to build a standard curve using the classical quantitative data analysis method. This could be attributed to different amplification efficiencies in different template dilution, which can be seen in the slope of each curve. A well-fitting standard curve was established if we drew the curve using other published theory[32-35], as shown in Fig. S4. However, since we may use different amounts of SYBR Green dye in different experiments, it is impossible to determine a universal paradigm as can be found in the traditional method.

Determination of influential factors of small MBs suitable for SMB-NEMA

It is acknowledged that improvements in NEMA efficiency will proceed from two directions: improvement of enzyme activity and optimization of thermodynamic parameters between small MBs and template. We have successfully improved enzyme activity by prohibiting *de novo synthesis*. On the other hand, small molecular beacons exist in different forms under stable temperature (step IV in Fig. 1). Thus, it is necessary to evaluate that thermodynamic data for molecular beacon, template and their duplex. What we discuss in this part is melting temperature (Tm) and free energy (ΔG^o).

In order to investigate the influence of melting temperature on reaction, we first determined the real melting temperature of small MBs. Referring to established theory, there are four commonly used methods to calculate melting temperature of a short sequence (Table 2). Tm of a long sequence based on nearest-neighbour interactions was close to the experimental data. However, it was not assisted in our small MBs selection. Referring to the multistate model (step IV in Fig. 1), all MB calculations are close to practical data. It should also be noted that under the stable temperature, inner primers and small MBs should have similar Tm to reaction temperature, indicating the importance of an identical temperature for small MBs, primers and reaction (Fig. S5). A similar result was also got as we optimized the number of base pair of small molecular beacon (Fig. S6)

In addition to melting temperature, hybridization between small MBs and template could be dependent on the tendency to bind to the target sequence. Thus we simulated small MBs hybridization activity under an isothermal condition (Fig. 6). In the absence of target (Fig. 6A), small MBs behaved as the theory predicted[33], except for a gradual RFU decrease at high temperature. This could be explained by random-coiled MBs winding to a close distance between the fluorophore and quencher. Calculations of melting temperature supported our hypothesis that MBs with Tm close to the reaction temperature perform better in SMB-NEMA (see Supplementary Information). In the presence of template (Fig. 6B), low Tm MBs bind to template and dissociate from target gradually before transforming to a random coil. After calculation (Fig. 7. see Supplementary Information), a small MB with 60°C melting temperature from these profiles was selected (Table 3),

Thus a different but similar designing rule for small molecular beacon was formed, mainly paying following attentions. First, Tm is the principal factor in small molecular beacon design, and the optimal annealing temperature for a reaction may actually be several degrees (1-2°C) above or below that of the Tm of primers, which is different from the traditional one that molecular beacons with Tm 10-15°C higher than the reaction temperature. Although the number of bases can also affect the hybridization of probe and target[15], it was not observed in our experiment. Second, judging rules of melting temperature and hybridization stability is different than the traditional method. Single-stranded DNAs are actually folded molecules, and this folding must be broken before binding, particularly for the loop-stem structure, which is not catered to the classical two-state theory[36,37], as indicated in Fig. 1 (step IV). Computations with a two-state model may be misleading in predicting performance of molecular beacons. A special molecular beacon has a ΔG increment owing to its special loop structure in a multistate model, therefore reducing temperature of unwinding[38-41]. Data provided by primer software to evaluate melting temperature can be inadequate, and needs to be corrected under the new algorithm in a multistate model.

Advantage of SMB-NEMA to other techniques

Compared to the previously widely reported PCR methods based on FRET, SMB-NEMA can accomplish equivalent sensitive target detection. Fig. S7 provided a representation of molecular beacon-based qPCR *Bacillus cereus* quantification. Results showed that qPCR can achieve about one copy number limit of quantification. Compared to qPCR, sensitivity of SMB-NEMA is not inferior to conventional qPCR, and it is the first time that SMB is developed in isothermal quantification based on the whole genome. Furthermore, SMB-NEMA is conducted in 20 minutes and finished within 50 minutes, which is much faster than

conventional qPCR. The practical samples test offered the similar results. 10 samples were collected and tested through SMB-NEMA and qPCR, and five were identified as contaminated (Table S2). This consequence is correct and matched to the traditional culture method (data not shown), which indicates SMB-NEMA application in food pathogens detection.

Tendency is showed to develop nicking endonuclease into isothermal quantitative method, some of which is similar to our SMB-NEMA. Joneja and Huang reported a linear nicking endonuclease-mediated strand-displacement DNA amplification, but it needs extra adapter ligation[42]. Schaerli also developed T4 replisome-based amplification technique to achieve quantitative detection based on the whole genome[43]. Connolly and Trau[44,45] once reported an isothermal method based on beacon-assisted amplification with simplicity and high sensitivity, it cannot be available rapidly on the whole genome. It has been reported that isothermal reaction based on the whole genome with nicking endonuclease has been limited by the reaction time[46]. SMB-NEMA achieve sensitive detection based on the practical samples and is much more applicable in food safety detection.

Conclusions

Herein, we have for the first time developed SMB-NEMA method to quantitatively detect nucleic acid target. After our optimization, SMB-NEMA can achieve sensitive and accurate detection without pollution. *De novo synthesis* is prohibitive to improve inherent specificity; Amplification based on the whole genome was achieved under the interference of other unrelated targets; Mismatched primers and beacons cannot make successful amplification. Accurate detection can be obtained from 3 copies limit of quantification (LOQ). Our method can also avoid opening the tube cover to prohibit pollution, which is a troublesome problem in isothermal amplification detection.

With the help of small molecular beacons, SMB-NEMA can be transplanted to a lateral flow strip. This type of strip will transform the fluorescence labelled in the amplified target to a visual colour in the reaction line[47-49]. Workers on site, such as those from The Agency of Inspection and Quarantine, will benefit from this visual improvement. Moreover, advances in point-of-care diagnosis will be faster under SMB-NEMA. Therefore, SMB-NEMA will achieve an unprecedented development towards visual and quantitative detection. Meanwhile, our method can be developed in combination with biosensors and functional nucleic acids, like DNAzyme and aptamer. Biosensors with our method will transmit more sensitive signal in a more convenient vehicle [50-52].

Acknowledgements

This work was supported by the Beijing New-star Plan of Science and Technology [xx2014B069]. Funding for open access charge: Beijing Council of Science and Technology. We herein thank Jing He and Wenying Tian for experimental guidance and their comments on the manuscript.

References

1. L. Yan, J. Zhou, Y. Zheng, A. S. Gamson, B. T. Roembke, S. Nakayama, and H.O. Sintim, *Mol. Biosyst.*, 2014, 10, 970-1003.
2. C. Duarte, E. Salm, B. Dorvel, Jr. B. Reddy and R. Bashir, *Biomed. Microdevices.*, 2013, 15, 821-830.
3. P. J. Asiello and A. J. Baeumner, *Lab Chip*, 2011, 11, 1420-1430.
4. L. Chen, J. Guo, Q. Wang, G. Kai and L. Yang, *J. Agri. Food Chem.*, 2011, 59, 5914-5918.
5. H. Kong, L. S. Higgins, M. A.Dalton, R. B. Kucera, I. S. Schildkraut, G. G. Wilson, United States patent US 0, 211, 506. 2003, Nov. 13.
6. T. Notomi, H. Okayama, H. Masubuchi, T. Yonekawa, K. Watanabe, N. Amino, and T. Hase, *Nucleic Acids Res.*, 2000, 28, e63; DOI: 10.1093/nar/28.12.e63.
7. M. Vincent, Y. Xu, and H. Kong, *EMBO Rep.*, 2004, 5, 795-800.
8. P. M. Lizardi, X. H. Huang, Z. R. Zhu, P. Bray-ward, D.C. Thomas and D.C. Ward, *Nat. Genet.*, 1998, 19, 225-232.
9. J. Jean, B. Blais, A. Darveau and I. Fliss, *Appl. Environ. Microb.*, 2001, 67, 5593-5600.
10. X. Liang, K. Jensen and M. D. Frank-Kamenetskii, *Biochemistry*, 2004, 43, 13459-13466.
11. P. T. Monis, S. Giglio, and C. P. Saint, *Anal. Biochem.*, 2005, 340, 24-34.
12. S. A. Bustin, V. Benes, J.A. Garson, J. Hellemans, J. Huggett, M. Kubista, R. Mueller, T. Nolan, M.W. Pfaffl, G.L. Shipley, J. Vandesompele and C.T. Wittwer, *Clin. Chem.*, 2009, 55, 611-622.
13. S. Tyagi and F. R. Kramer, *Nat. Biotechnol.*, 1996, 14, 303-308.
14. M. Nilsson, M. Gullberg, F. Dahl, K. Szuhai and A. K. Raap, *Nucleic Acids Res.*, 2002, 30, e66; DOI: 10.1093/nar/gnf065.
15. J. J. Li, Y. Chu, B. Y. Lee and X. S. Xie, *Nucleic Acids Res.*, 2008, 36, e36; DOI: 10.1093/nar/gkn033.
16. J. J. Li, R. Geyer and W. Tan, *Nucleic Acids Res.*, 2000, 28, e52; DOI: 10.1093/nar/28.11.e52.
17. J. D. Wang, X. H. Wang, Y. Li, J. K. Zhang and L. S. Zhan, *Mil. Med. Sci.*, 2012, 36, 65-69.
18. F.H. Stephenson, 2010, pp 165-185 Academic Press, New York.

19. Michael, A. I., David, H. G. and J.J. Sninsky. (1995) PCR Strategies. Ch. 6 pp 69–83, Academic Press, New York.
20. G. Bonnet, S. Tyagi, A. Libchaber and F. R. Kramer, *Proc. Natl. Acad. Sci.* U.S.A., 1999, 96, 6171-6176.
21. M. Zuker, *Nucleic Acids Res.*, 2003, 31, 3406-3415.
22. A. I. Michael, H. G. David, and J.J. Sninsky. 1995, pp 69–83, Academic Press, New York.
23. Jr. J. SantaLucia, *Proc. Natl. Acad. Sci.* U.S.A., 1998, 95, 1460-1465.
24. Jr, J. SantaLucia and D. Hicks, *Annu. Rev. Biophys. Biomol. Struct.*, 2004, 33, 415-440.
25. N. Peyret, 2000, PhD dissertation, Wayne State University, Department of Chemistry, Detroit, MI.
26. R. T. Koehler and N. Peyret, *Comput. Biol. Chem.*, 2005, 29, 393-397.
27. W. Henke, K. Herdel, K. Jung, D. Schnorr and S. A. Loening, *Nucleic Acids Res.*, 1997, 25, 3957-3958.
28. A. N. Spiess, N. Mueller and R. Ivell, *Clin. Chem*., 2004, 50, 1256-1259.
29. C. A. Heid, J. Stevens, K. J. Livak and P. M. Williams, *Genome Res.*, 1996, 6, 986-994.
30. K. Arumuganathan and E. D. Earle, *Plant Mol. Biol. Rep.*, 1991, 9, 208-218.
31. S. C. Huang, Y.C. Xu, X.H. Yan, Y. Shang, P. Y. Zhu, W.Y. Tian and W.T. Xu, *J. Sci. Food Agri.*, 2014, 95, 253-259.
32. R. G. Rutledge and D. Stewart, *BMC Biotechnol.*, 2008, 8, 47-50.
33. J. M. Ruijter, C. Ramakers, W.M.H. Hoogaars, Y. Karlen, O. Bakker, M.J.B. Van der Hoff, and A.F.M. Moorman, *Nucleic Acids Res.*, 2009, 37, e45; DOI: 10.1093/nar/gkp045.
34. A. Lievens, S. Van Aelst, M. Van den Bulcke and E. Goetghebeur, *Nucleic Acids Res.*, 2012, 40, e10; DOI: 10.1093/nar/gkr775.
35. T. Bar, M. Kubista and A. Tichopad, *Nucleic Acids Res*., 2012, 40, 1395-1406.
36. Jr. J. SantaLucia and D. H. Turner, *Biopolymers*, 1997, 44, 309-319.
37. Jr. J. SantaLucia, 2000, pp 134-144, Oxford Press, Oxford.
38. M. Zuker, *Nucleic Acids Res.*, 2003, 31, 3406-3415.
39. N. E. Watkins and Jr. J. SantaLucia, *Nucleic Acids Res.*, 2005, 33, 6258-6267.
40. Jr. J. SantaLucia, *Proc. Natl. Acad. Sci. U.S.A.*, 1998, 95, 1460-1465.
41. J. J. Jo, M. J. Kim, J. T. Son, J. Kim and J. S. Shin, *Biochem. Bioph. Res. Commun.*, 2009, 385, 88-93.
42. A. Joneja and X. Huang, Analytical biochemistry, 2011, 414, 58-69.
43. Y. Schaerli, V. Stein, M. M. Spiering, S. J. Benkovic, C. Abell, and F. Hollfelder, Nucleic Acids Res., 2010, 38, e201-e201.

44. A. R. Connolly and M. Trau, *Angew. Chem.*, 2010, 122, 2780-2783.

45. A. R. Connolly and M. Trau, *Nat Protoc.*, 2011, 6, 772-778.

46. T. Murakami, J. Sumaoka and M. Komiyama, *Nucleic Acids Res.*, 2009, 37, e19; DOI: 10.1093/nar/gkn1014.

47. H.F. Dong, C. Wang, Y. Xiong, H.T. Lu, H.X. Ju and X.J. Zhang. *Biosens. Bioelectron.*, 2013, 41, 348-353.

48. H.F. Dong, K.H. Hao, Y.P. Tian, S. Jin, H.T. Lu, S.F. Zhou and X.J. Zhang. *Biosens. Bioelectron.*, 2014, 53, 377-383.

49. H.F.Dong, S. Jin, H.X. Ju, K.H Hao, P.L. Xu, H.T. Lu and X.J. Zhang, *Anal. Chem.*, 2012, 84, 8670-8674.

50. C. Yang, V. Lates, S. B. Prieto, L. M. Jean and X. R. Yang, *Biosens. Bioelectron.*, 2012, 32, 208-212.

51. J. H. Chen and L.W. Zeng, *Biosens. Bioelectron.*, 2013, 42, 93-99.

52. Y. L. Yuan, S.Q. Wei, G.P. Liu, S.B. Xie, Y.Q. Chai, and R. Yuan, *Analytica chimica acta*, 2014, 811, 70-75.

Figure Legends

Figure 1 Schematic representation of the fluorescence mechanism of SMB-NEMA. The blue arrows indicate all process of amplification (I, II and III). The duplex target is amplified with S_1 /S_2 and $B_{1/}$ B_2 after denaturation, producing a new duplex with two nicking endonuclease recognition sites (Step I). Then, the extension strand falls into a cycle. S_1 /S_2 continue to generate a single strand displaced under the activity of Bst DNA polymerase (Step III). In this step, one extension strand will produce two identical amplicons, indicating the exponential amplification format. Small molecular beacons bind to complementary target to monitor real-time amplification process. In addition to this process, dNTPs in the reaction generate another strand with palindromic structure and high G-C content in the presence of nicking endonuclease and Bst DNA polymerase. (Step II). This phenomenon, as we called *de novo synthesis*, occurs in all processes of SMB-NEMA amplification. Small molecular beacons in the reaction act in dynamic equilibrium with three main states: completely folded (a), bound to target (b) and random coil (c). The first two are included in the two-state model (Step IV).

Figure 2. Optimization of NEMA reaction. Lanes 1-3 and 4-5 in Fig. 3A indicate *de novo synthesis* simulation with Nt. BstNBI and Nt. BspQI, respectively. Lanes 6-7 and 8-9 indicate NEMA amplification with Nt. BstNBI and Nt. BspQI, respectively. Each condition is outlined in duplicate, except *de novo synthesis* condition with Nt. BstNBI is outlined in triplicate. Primers and targets used in this reaction are shown in Table S1. Lanes 1-10 in 3B indicate betaine optimization in the presence of the whole genome with addition of 0.5, 1, 1.5, 2, and 2.5 M, respectively. Each condition is outlined in duplicate in the figure. Lanes 1-10 in 3C indicate trehalose optimization in the presence of whole genome with the addition of 40, 50, 60, 70, and 80 mM, respectively. Lane M contains maker DL2000 in both figures. Each condition is outlined in duplicate in the figure.

Figure 3. Amplification curve of different molecular beacons. Letters A-F represent NEMA with addition of molecular beacons with Tm of 75°C, 70°C, 65°C, 60°C, 55°C, and 50°C, respectively. The X-axis stands for number of cycles, and the Y-axis stands for fluorescence value (RFU). All experiments were performed and outlined in duplicate, except negative control that performed in duplicate and outlined in one curve for comprehensive appearance.

Figure 4. Molecular beacon performance with different additions in NEMA. Letters A-D represent real-time amplification curve (blue) and Letters E-H represent the standard curve between the logarithm of the initial template DNA concentration and the Ct value, respectively. Negative controls (red) were also included. The best linear correlation is indicated in the Figure. without poorly-behaving amplification curves. A, B and D were established from 200 ng/μL to 0.01 ng/μL; C was established from 200 ng/μL to 1 ng/μL. All experiments were performed and outlined in duplicate, except negative control that performed in duplicate and outlined in one curve for comprehensive appearance.

Figure 5. (A) Sensitive quantification of NEMA based on small molecular beacon. Ten-fold dilution templates (blue) are presented by three parallels, with negative control (red) included. (B)Linear regression curve between the logarithm of the initial template DNA concentration and the Ct value. Dotted square (■), dotted circle (●) and dotted triangle (▲) stand for three parallels of each dilution group. The slope and Y-intercept were -3.22 and 52.92, respectively. The linear correlation coefficient (R2) is 0.975. All experiments were performed and outlined in duplicate, except negative control that performed in duplicate and outlined in one curve for comprehensive appearance.

Figure 6. Thermodynamic melting curve of MBs in NEMA simulated condition. (A) Melting curve of MBs in the absence of template. MBs of Tm at 75°C (yellow), 70°C (green), 65°C (red), 60°C (pink), 55°C (blue) and 50°C (orange) were conducted by at least two parallels. (B) Melting curve of MBs in the presence of template. MBs shown are those of Tm at 75°C (yellow), 70°C (green), 65°C (red), 60°C (pink), 55°C (blue) and 50°C (orange).

Figure 7. Increase in the melting temperature of the MBs–template duplex that results from increasing the concentration of target oligonucleotides was used to determine the thermodynamic parameters that describe the dissociation of duplex. The slope of each fitted line is equal to the negative value of the enthalpy and the intercept is equal to the entropy.

Table 1. Scheme of primers and molecular beacons

Sequence function	Sequence name	Sequence (5'-3')	Reference
16s rDNA	16s-F	AACGCTGGCGGCGTGCCTAA	This study
	16s-R	CCTTCCGATACGGCTACCTTGTTA	
B. cereus outer primer	B_1	CCAGACTCCTACGGGAGGCAGCAGT	17
	B_2	GTTTACGGCGTGGACTACCAGGGTA	
B. cereus inner primer	S_1	ATGAATAGTCGGTTACTTGAGTCTCCGCAATGGACGAAAGTCT	
	S_2	ATGAATAGTCGGTTACTTGAGTCCTTGCCACCTACGTATTACC	
molecular beacon	Beacon-75	CTCGAGCGTGAGTGATGAAGGCTTTCTCGAG	This study
	Beacon-70	CTCGACGTGAGTGATGAAGGCTTTTCGAG	
	Beacon-65	CTCGAGTGAGTGATGAAGGCTTCGAG	
	Beacon-60	CTCGAGAGTGATGAAGGCTCGAG	
	Beacon-55	CTCGAGTGATGAAGGTCGAG	
	Beacon-50	CTCGAGAGTGATGATCGAG	
	Beacon-60 M	CTCGAGAGTGATCAAGGCTCGAG	

Table 2. Melting temperature (T_m) based on different algorithms

	Basis	Formula	Reference
1	Number of bases	T_m = 2℃ (A+T)+4℃ (G+C)	18
2	G/C content, DNA length and salt concentration	$Tm = 81.5 + 16.6\log\left[\frac{[SALT]}{1+0.7[SALT]}\right] + 0.41(\%G+C) - \frac{500}{L}$	19
3	Nearest-neighbor interactions in two-state model	$Tm = \frac{T\Delta H}{\Delta H - \Delta G + RTln(C)} + 16.6\log\left[\frac{[SALT]}{1+0.7[SALT]}\right] - 269.3$	19
4	Multistate model	Tm is the temperature at which K_{12} equals T-0.5B	20

Table 3. Melting temperature of MBs based on different algorithms.

	T_m calculations						ΔG calculations	
MB name	T_{m1} [a]	T_{m2} [b]	T_{m3} [c]	T_{m4} [d]	T_{m5} [e]	T_{m6} [f]	Estimated	Practical
beacon-75	74.9	100	75.78	74.74	69	70.11	-13	1.9
beacon-70	70	88	73.78	72.51	66	67.53	-11.9	-1.2
beacon-65	65.4	80	72.66	69.16	64	63.98	-10.7	-0.9
beacon-60	61.5	72	71.25	67.03	58	59.67	-8.5	-2.9
beacon-55	56.2	62	67.37	61.74	51.5	52.31	-5.6	—[g]
beacon-50	49.9	58	65.08	59.24	51.5	51.12	-3.7	—[g]

a T_{m1} stands for the melting temperature of MB in the software.

b T_{m2} stands for the melting temperature of MB in method 1.

c T_{m3} stands for the melting temperature of MB in method 2.

d T_{m4} stands for the melting temperature of MB in method 3.

e T_{m5} stands for the melting temperature of MB in experiment (more details are listed in Figure S3).

f T_{m6} stands for the melting temperature of MB in method 4.

g — indicates that data are unavailable from the experiment.

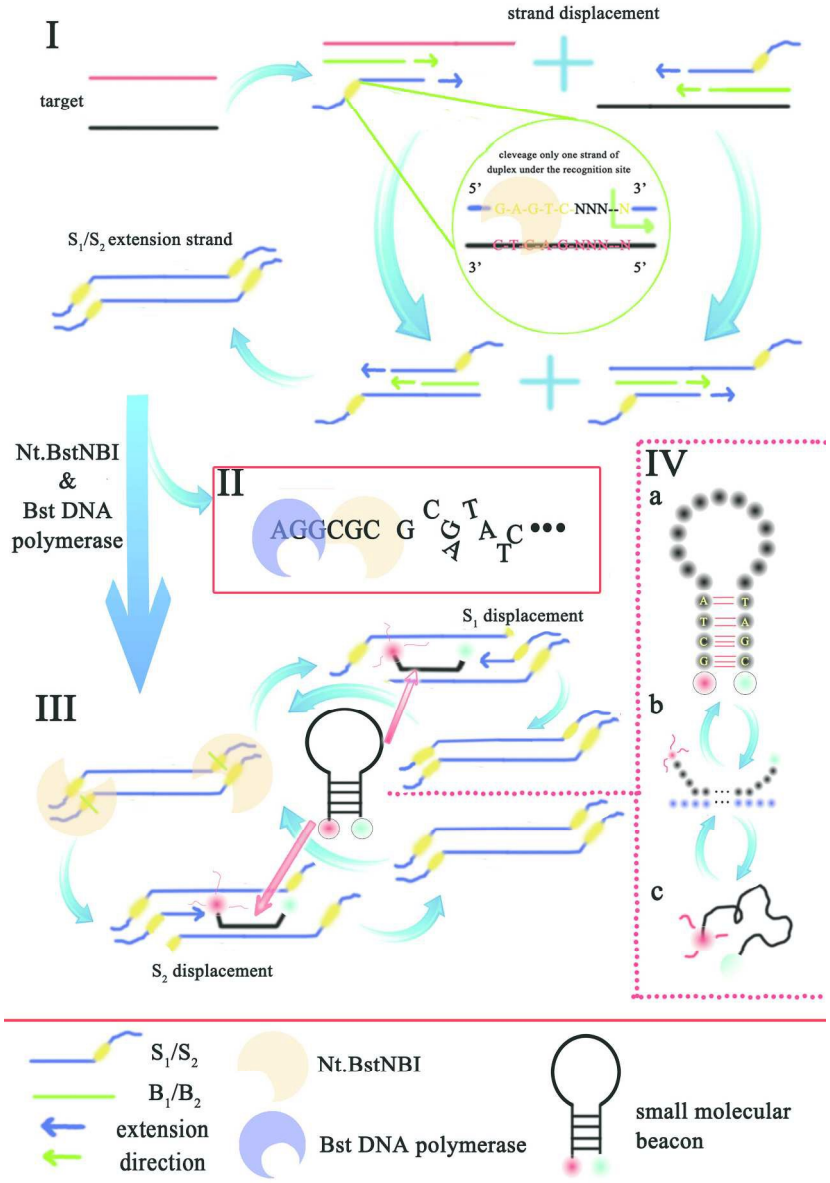

177x260mm (300 x 300 DPI)

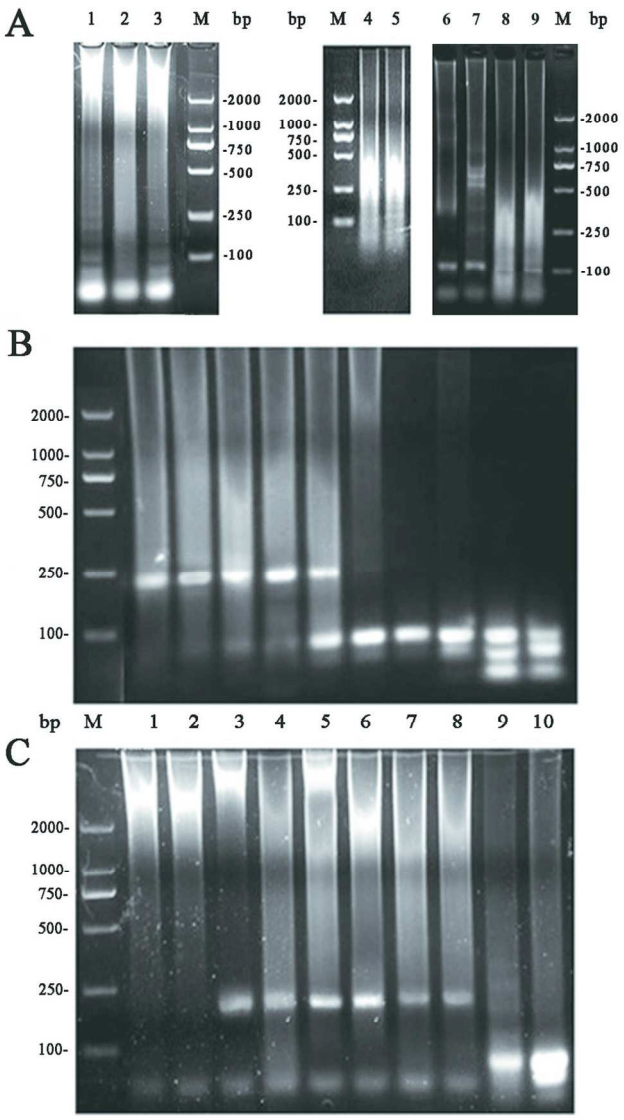

83x150mm (300 x 300 DPI)

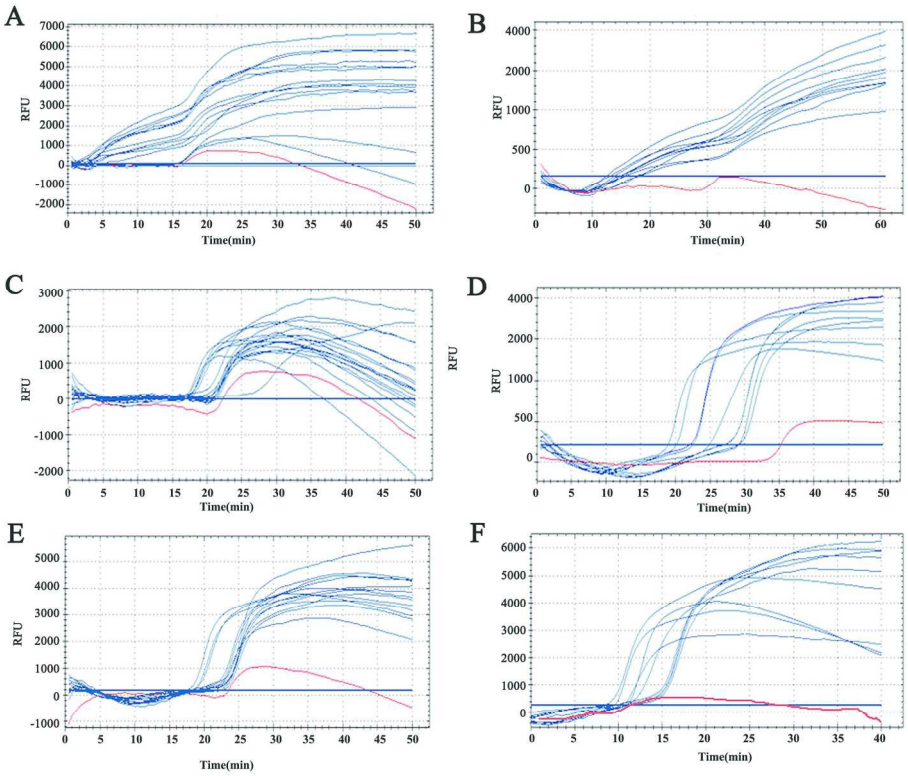

177x150mm (300 x 300 DPI)

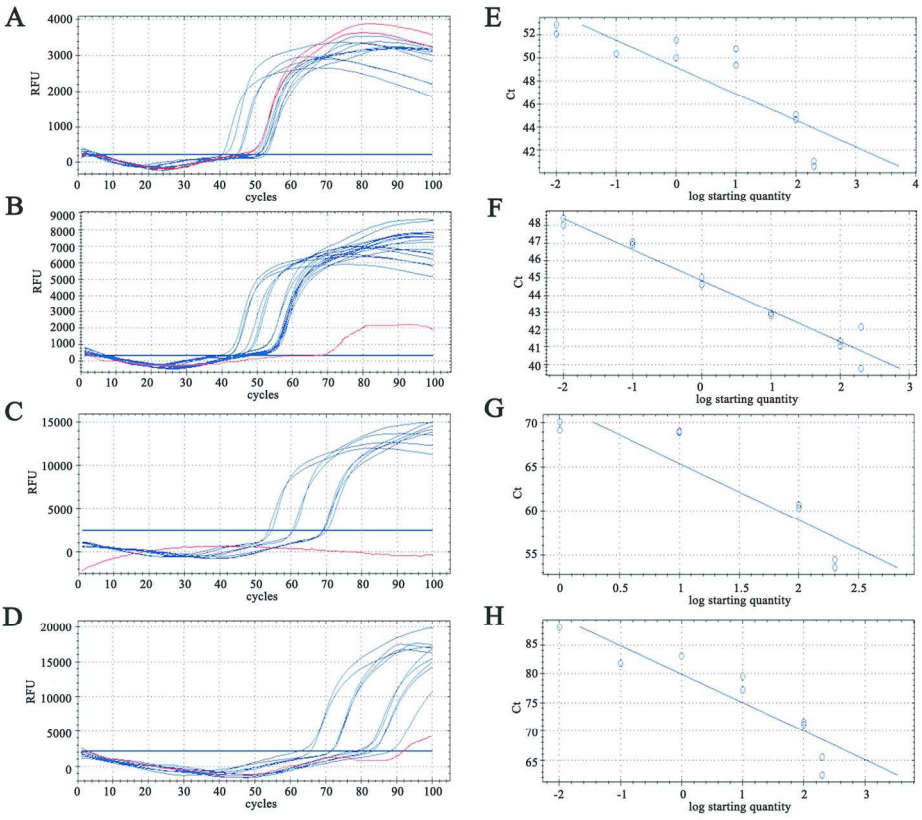

177x150mm (300 x 300 DPI)

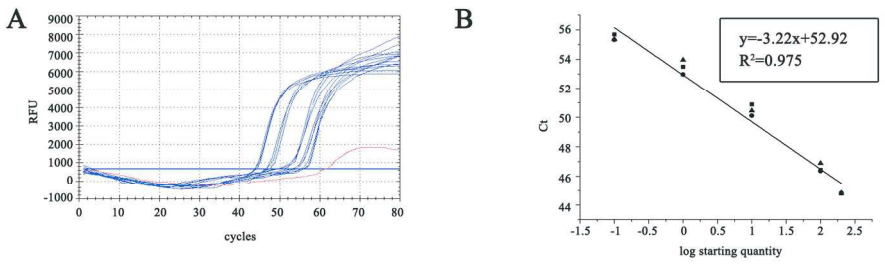

177x50mm (300 x 300 DPI)

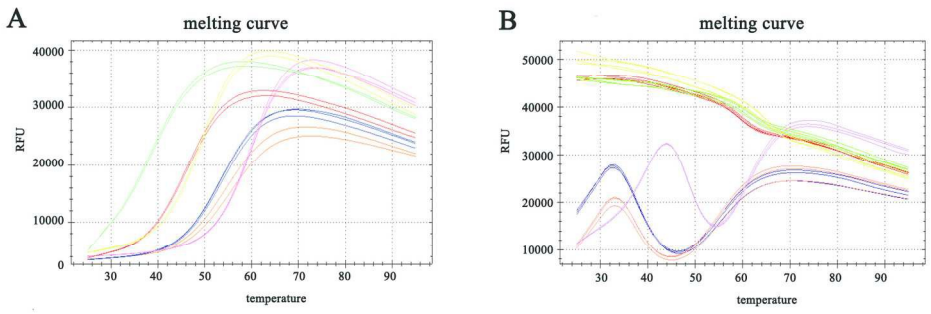

177x60mm (300 x 300 DPI)

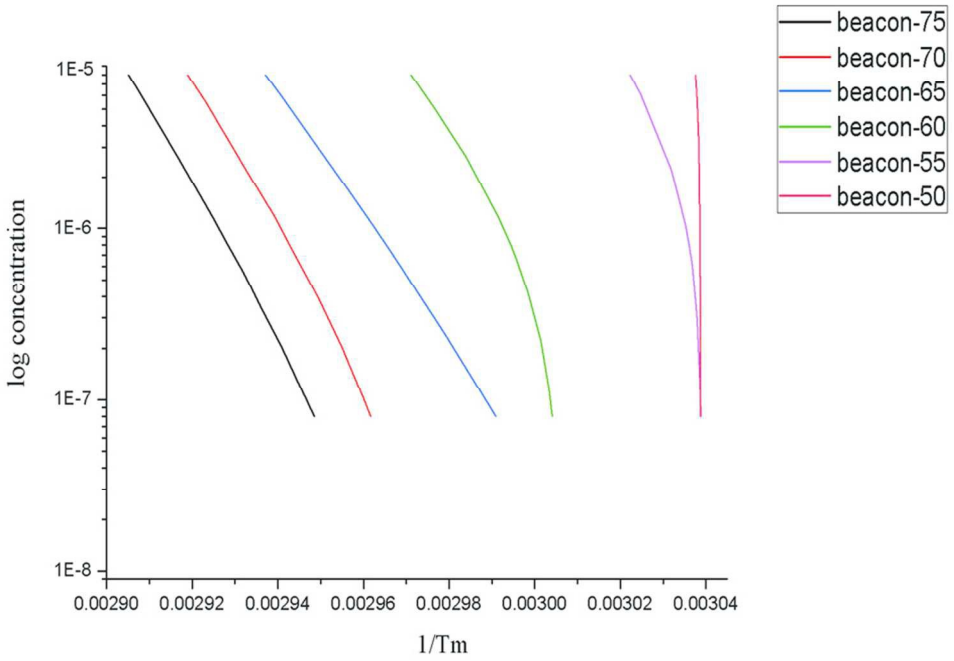

83x60mm (300 x 300 DPI)